Published in final edited form as:
Circ Res. 2011 October 14; 109(9): 1055–1066. doi:10.1161/CIRCRESAHA.111.253955.

Human Atrial Action Potential and Ca^{2+} Model: Sinus Rhythm and Chronic Atrial Fibrillation

Eleonora Grandi, Ph.D.[1,*], **Sandeep V. Pandit, Ph.D.**[2,*], **Niels Voigt, M.D.**[3,*], **Antony J. Workman, Ph.D**[4], **Dobromir Dobrev, M.D.**[3], **Jose Jalife, M.D.**[2,**], and **Donald M Bers, Ph.D**[1,**]

[1]Department of Pharmacology, University of California at Davis, Davis, CA, USA

[2]Center for Arrhythmia Research, University of Michigan, Ann Arbor, MI, USA

[3]Division of Experimental Cardiology, Medical Faculty Mannheim, University of Heidelberg, Mannheim, Germany

[4]Institute of Cardiovascular and Medical Sciences, University of Glasgow, UK

Abstract

Rationale—Understanding atrial fibrillation (AF) requires integrated understanding of ionic currents and Ca^{2+} transport in remodeled human atrium, but appropriate models are limited.

Objective—To study AF we developed a new human atrial action potential (AP) model, derived from atrial experimental results and our human ventricular myocyte model.

Methods and Results—Atria vs. ventricles have lower I_{K1}, resulting in more depolarized resting membrane potential (~7mV). We used higher $I_{to,fast}$ density in atrium, removed $I_{to,slow}$, and included an atrial-specific I_{Kur}. I_{NCX} and I_{NaK} densities were reduced in atrial vs. ventricular myocytes according to experimental results. SERCA function was altered to reproduce human atrial myocyte Ca^{2+} transients. To simulate chronic AF, we reduced I_{CaL}, I_{to}, I_{Kur} and SERCA, and increased I_{K1}, I_{Ks} and I_{NCX}. We also investigated the link between Kv1.5 channelopathy, $[Ca^{2+}]_i$, and AF. The sinus rhythm model showed a typical human atrial AP morphology. Consistent with experiments, the model showed shorter APs and reduced AP duration shortening at increasing pacing frequencies in AF or when I_{CaL} was partially blocked, suggesting a crucial role of Ca^{2+} and Na^+ in this effect. This also explained blunted Ca^{2+} transient and rate-adaptation of $[Ca^{2+}]_i$ and $[Na^+]_i$ in chronic AF. Moreover, increasing $[Na^+]_i$ and altered I_{NaK} and I_{NCX} causes rate-dependent atrial AP shortening. Blocking I_{Kur} to mimic Kv1.5 loss-of-function increased $[Ca^{2+}]_i$ and caused early-afterdepolarizations under adrenergic stress, as observed experimentally.

Conclusions—Our study provides a novel tool and insights into ionic bases of atrio-ventricular AP differences, and shows how Na^+ and Ca^{2+} homeostasis critically mediate abnormal repolarization in AF.

Keywords

computer model; action potential; Ca^{2+} cycling; atrial fibrillation

Correspondence: Donald M Bers, Ph.D., Department of Pharmacology, University of California, Davis, 451 Health Sciences Drive, GBSF Room 3513, Davis, CA 95616-8636, Phone:+1 (530) 752-6517, Fax: +1 (530) 752-7710, dmbers@ucdavis.edu.
*E.G., S.V.P., and N.V. contributed equally to this work
**J.J. and D.M.B. share senior authorship

Disclosures None.

Introduction

Atrial fibrillation (AF) is the most common cardiac arrhythmia observed clinically, and is the main cause of embolic stroke [1]. The mechanisms underlying AF remain unclear, and AF is thought to be maintained either via ectopic foci, multiple wavelets, or fibrillatory conduction emanating from a small number of stable rotors [2]. Electrical and structural remodeling have emerged as key elements in the development of the AF substrate (e.g., the tendency for persistence of AF)[3]. Electrical remodeling includes changes in Ca^{2+} and K^+ currents leading to shortening of the action potential (AP) duration (APD) and loss of APD rate-dependent adaptation, whereas structural remodeling leads to changes in atrial myocyte and tissue morphology (e.g. cell hypertrophy, fibrosis) [3-5].

At present mechanisms leading to perpetuation of AF are still undetermined. Growing experimental evidence points to abnormal intracellular Ca^{2+}-handling as a key mediator in AF-pathophysiology [6, 7], but the mechanism through which Ca^{2+}-related abnormalities can lead to the occurrence and maintenance of AF are poorly understood. Models of human atrial myocytes have been developed and used to gain mechanistic insights into human atrial cell physiology and pathophysiology [8-10], however none of these included detailed descriptions of Ca^{2+} (or Na^+) regulatory processes. A recent simulation study incorporated and studied the sub-cellular nature of Ca^{2+} homeostasis and its relation to human atrial action potentials [11]; however the role of Ca^{2+} in mediating AF was not investigated.

We recently developed a model of the human ventricular myocyte AP and Ca^{2+} transient (CaT) [12], a major advance over prior human ventricular models in robustly describing excitation-contraction coupling, and the model was extensively validated against a broad range of experimental data.

The aims of the present study were two fold: 1) to derive a new human atrial cell model with detailed Ca^{2+} handling, by implementing experimentally documented structural and ionic differences in atrial vs. ventricular cells [13] and starting from our recently published model of human ventricular myocytes[12]; 2) to study how Ca^{2+} homeostasis is involved in abnormal APs seen in chronic AF (cAF), and AF related to adrenergic stress in patients with Kv1.5 mutations [14]. Ionic currents in the ventricular model were modified based on experimental data comparing protein expression and function in atrial vs. ventricular myocytes. Importantly, we utilized new experimental data addressing the poorly understood molecular basis of impaired atrial Ca^{2+} signaling in cAF to constrain our model parameters.

We validated our model by testing its ability to recapitulate a wide range of physiological behaviors observed in experiments. We next investigated the mechanisms of APD and CaT rate-adaptation in sinus rhythm and cAF, and assessed the effects of blocking the atrial-specific ultrarapid K^+ current (I_{Kur}) in the absence and presence of β-adrenergic activation, to understand arrhythmogenesis in AF related to Kv1.5 channelopathy and adrenergic stress. Finally, right-to-left gradients in repolarizing currents were also included in the model, since in a number of instances the driving source of the AF (reentry or foci) is located in the left atrium [2].

Methods

Cellular $[Ca^{2+}]_i$ and electrophysiological methods are described in the Online Supplement and were used to tune our model and for validation. Table 1 shows key changes made in our new human atrial model vs. our ventricular myocyte model, [12] to account for ionic remodeling in cAF, and to simulate the effects of β-adrenergic and cholinergic stimulation. Further details are in Online Supplement, including formulation of I_{Kur} block by AVE0118.

Model differential equations were implemented in Matlab (Mathworks Inc., Natick, MA, USA) and solved numerically using a variable order solver (ode15s). APDs were obtained after pacing digital cells at indicated frequencies at steady-state. APD was measured as the interval between AP upstroke and 90% repolarization level (APD_{90}).

Results

The baseline alterations to our ventricular cell model resulted in a typical Type-3 human atrial AP morphology[15] (Figure 1A, right panel). The higher density of K^+ currents that are active in AP phase 1 (early repolarization, I_{to}+I_{Kur}) confers the AP a triangular shape lacking a plateau phase. We have investigated the impact on AP shape of varying I_{to} and I_{Kur} densities, and quantified the changes in the plateau potential, which gets more depolarized as the degree of K^+ channel blockade increases (Online Figure I, Online Supplement). AP waveform also feeds back onto ion channel gating determining notable differences in atrial currents. For example, although atrial I_{to} is almost twice as large in voltage clamp experiments (see Online Figure II), in current clamp conditions it is comparable to ventricular $I_{to,fast}$ (Figure 1G, right vs. left panel). Maximal velocity of AP upstroke was comparable to that measured in experiments of ~140 V/s (vs. 250 V/s in cAF) [16], and was smaller than in the ventricular cell model (372 V/s in the epicardial cell model paced at 1 Hz [12]). In fact, I_{Na} is remarkably reduced in atrial vs. ventricular cells (Figure 1C, right vs. left panel) during the AP, due to more inactivated channels (because of slower recovery from inactivation at more depolarized atrial resting membrane potential). Although I_{Kr} or I_{Ks} were not modified vs. ventricular myocytes, the spiky AP reduced net I_{Kr} and I_{Ks} (Fig. 1E and F). It is noteworthy that the reduction of I_{NCX} from the ventricular model resulted in larger I_{NCX} in the atrial model (Fig. 1K). This is presumably because of the short early repolarization in atrium and the slightly larger CaT, both favoring inward I_{NCX}. I_{CaL} is similar in atria and ventricle in voltage-clamp conditions, but the AP shape causes I_{CaL} to be much larger in atrial vs. ventricular myocyte model (Fig. 1D). I_{K1} is smaller in atria, consistent with its lower maximal conductance. I_{NaK} is decreased (not as much as its pump rate because the higher $[Na^+]_i$, 9.1 in atrium vs. 8.2 mmol/L in ventricle at 1 Hz pacing rate, activates the pump more).

A typical Ca^{2+} transient is shown in Figure 1B (right panel): at 1 Hz pacing rate, diastolic $[Ca^{2+}]_i$ is 207 nmol/L and peaks at 462 nmol/L. Simultaneous I_{CaL} and $[Ca^{2+}]_i$ measurements in human atrial myocytes at physiological temperature are shown in Figure 2D-G and compared to simulated traces (Figure 2A-B; 0.5 Hz). Simulated CaT amplitude and rate of CaT decay matched the experimental data (Fig. 2B grey line vs. E, and Fig. 2H-I), as did peak I_{CaL} (-6.47 A/F vs. -6.78±0.36 in experiments, Fig. 2A grey line vs. D). When cAF was simulated, by accounting for ion channel remodeling as illustrated in the methods, I_{CaL} was greatly diminished (Fig. 2A, black vs. grey lines), as shown in experiments (Fig. 2D vs. F) [4, 17, 18]. The reduced I_{CaL} could explain the reduced sarcoplasmic reticulum (SR) Ca^{2+} release and CaT amplitude (Fig. 2B,E,G,H), even if SR Ca^{2+} content were unaltered. However, the reduced I_{CaL} and SERCA function (rate of twitch $[Ca^{2+}]_i$ decline; Fig. 2I) and the elevated SR Ca^{2+} leak and NCX function (greater I_{NCX} for a given $[Ca^{2+}]_i$; Fig. 3A-G) all tend to lower SR Ca^{2+} content in cAF, which is apparent in the model (but not significantly so in the experiments; Fig. 3H).

We next tested the response of our model to changes in pacing frequency. Simulated human atrial cell APs under baseline conditions (Fig. 4D) shorten with faster pacing rates (Figure 4J, black circles) as shown in atrial myocytes from patients in normal sinus rhythm (Fig. 4A and 4M, black circles) [19]. To illustrate the effect of a reduction in I_{CaL} Van Wagoner *et al.* [19] recorded APs from the same myocytes at various cycle lengths in the presence of the I_{CaL} blocker nifedipine (10 μM), showing little rate–dependent change in APD (Fig. 4C and

4M, grey open circles). Li and Nattel [20] obtained analogous results. Similarly, simulated APs following 50% I_{CaL} block (Figure 4F) exhibited impaired APD rate-adaptation (Figure 4J, grey open circles). Myocytes from chronic AF patients (Figure 4B) are characterized by shorter APD_{90} values [16, 19, 21-23], with less variation as a function of cycle length than control (sinus rhythm) myocytes (Figure 4M, squares) [4, 16, 19, 22, 23]. Analogously, our cAF model predicts shorter APs than sinus rhythm (solid vs. dashed line in Fig. 4D *inset*), and reduced adaptation to changes in pacing frequency (Figure 4J, squares). At 4 Hz pacing AP duration alternates (Fig. 4E, and so does $[Ca^{2+}]_i$ in Fig. 4H). The sinus rhythm model exhibits this behavior at higher frequency (Fig. 4O at 6 Hz pacing rate).

The model predicts a positive dependency of CaT amplitude on the pacing rate in sinus rhythm (Figure 4G and K, black circles), which is in agreement with intracellular $[Ca^{2+}]$ measurements via aequorin light signals (Figure 4N, grey circles and dashed line) [24] and twitch force measurements (Figure 4N, open circles and solid line) [24, 25]. Positive dependency is impaired when I_{CaL} is partially inhibited (Figure 4F and K, grey open circles) and in cAF (Figure 4E and K, squares). Similarly, atrial myocytes from patients with cAF show impaired contractility (Figure 4N, squares)[25]. Our model also predicts the increase of intracellular $[Na^+]$ with increasing pacing frequency, as shown in Figure 4L (and Online Figure IIIA), which is more limited in cAF and with inhibition of I_{CaL} compared to sinus rhythm (squares and grey open circles vs. black circles).

Figures 5 and Online Figure III show that $[Na^+]_i$ is critical for APD rate-adaptation. Time courses of APD_{90} and $[Na^+]_i$ changes subsequent to an increase in pacing frequency from 0.5 to 1 Hz (Online Figure IIIC) suggest that non steady-state measurements (before $[Na^+]_i$ slowly reaches steady-state) may give rise to highly variable experimental APD adaptation curves. Moreover, if $[Na^+]_i$ is clamped in the model, the APD rate adaptation is nearly abolished (Fig. 5A). Simulation of partial block of NKA causes a biphasic APD response (Figure 5D): first, APD prolongation by acute NKA current block, then as $[Na^+]_i$ rises it increases outward NKA causing APD shortening. Importantly, we validated these model predictions in isolated human atrial myocytes challenged with strophanthidin (10 μmol/L). Acute NKA inhibition was confirmed by abrupt and relatively sustained depolarization of resting membrane potential (Figure 5C). Figure 5C shows a typical time course of APD_{90} from a representative cell and pooled data (n=10). Strophanthidin application produces an initial marked increase and subsequent decrease in APD_{90} (Figure 5C, right). Similar behavior has been described in guinea pig ventricular myocytes, [26] human atrial fibers, [27] and rabbit atrial myocytes (not shown).

Blockade of the atrial specific current I_{Kur} has been proposed to improve atrial contractility without increasing the risk of ventricular arrhythmias. In fact, in human atrial myocardium, block of I_{Kur} results in a prolongation and elevation of the AP plateau, which elicit a positive inotropic effect [28, 29]. Thus, we assessed the impact of I_{Kur} block (modeled as shown in Online Methods and Online Figure IV) on APD and CaT (Figure 6 and Online Figure V). Moderate blockade of I_{Kur} (by 25-50%) increases CaT amplitude (Figure 6B) with little effects on APD (Figure 6A) both in sinus rhythm and cAF models, in agreement with experimental results (Figure 6A and B, *insets*) [28, 29]. Enhancement of CaT amplitude is greatly increased when I_{Kur} is more fully (75-100%) blocked (Figure 6B), paralleled by AP prolongation (Figure 6A) in agreement with [14] (see also Figure 6D, *inset*). A more moderate increase in CaT amplitude is also predicted in cAF. In Figure 6C the predicted impact of various degrees of I_{Kur} block on sinus rhythm and cAF CaT amplitude (grey symbols and axis) shows good agreement with the reported effect of the I_{Kur} inhibitor AVE0118 on contractile force of atrial trabeculae from patients in sinus rhythm and in AF (black symbols and axis) [29].

To study AF associated with Kv1.5 mutation during β-adrenergic activation, we also investigated the effect of adrenergic stimulation on atrial AP (Figure 6D) by incorporating steady-state effects of PKA-dependent phosphorylation on I_{Ca}, I_{Ks}, I_{Kur}, PLN-SERCA2a, RyR2, troponin Ca^{2+} affinity and Na/K-ATPase (see Online Supplement). In our simulations, administration of isoproterenol (ISO) causes the CaT amplitude to increase (by ~ 65%, not shown) without major changes in the duration of repolarization (Figure 6D, solid black vs. blue lines), in agreement with data from human atrial preparations [30]. When simulating the block of I_{Kur} (which is enhanced during adrenergic activation) in the presence of ISO, early after-depolarizations (EADs) occurred (Figure 6D, green dashed line). These results are in agreement with data from Olson *et al*. [14] (Figure 6D, *inset*) showing that 4-AP (50 μmol/L) prolonged APD in human atrial myocytes and caused EADs and triggered activity upon ISO (1 μmol/L) challenge. Notably, simulation of I_{Ks} (also increased by ISO) blockade (50%) did not affect atrial AP markedly (Figure 6D, red line almost completely overlaps black line).

To reflect parasympathetic effects we also now include an I_{KACh} model (fitted with human data) and demonstrate a dose-dependent reduction in human atrial AP and CaT in response to the parasympathetic transmitter acetylcholine (Online Figure VI). The APD shortening is consistent with experiments in human atria. We did not integrate crosstalk between β-adrenergic and acetylcholine or CaMKII pathways, or develop compartmentalized dynamic G-protein coupled receptor models as done recently for animal myocyte models,[31,32] but those would be a logical extensions of our model.

There is only limited data available concerning intra-atrial heterogeneities in repolarizing currents in human atrial myocytes. Caballero *et al*. found a gradient of I_{Kur} with 20% higher density in right atrium (RA) vs. left atrium (LA) [33]. We incorporated such heterogeneity to simulate RA and LA APs and CaT (Figure 7A). The slightly higher I_{Kur} density in RA has negligible effects on AP and mildly decreases CaT amplitude (Fig. 7A, left; see also Fig. 6). cAF decreases I_{to} and I_{Kur} differentially in right vs. left atrium [33]. Indeed, cAF greatly reduced I_{to} in the RA (~80%) and to a lesser extent in the LA (~45%), thus generating RA-LA I_{to} gradient. In contrast, I_{Kur} was more markedly reduced in the RA (-55%) than in the LA (-45%), thus abolishing the atrial right-to-left I_{Kur} gradient observed in sinus rhythm. We simulated these perturbed left-to-right gradients in cAF. I_{K1} in LA was 2-fold higher in both paroxysmal AF and cAF than in SR, with a left-to-right gradient in paroxysmal AF only [34]. Thus, we did not simulate such gradient here. The model predicted a longer AP in the RA during cAF, similar to experimental data [35], with slightly larger CaT amplitude (Figure 7A, right, solid vs. dashed lines), but reduced APD adaptation (Figure 7A, right, solid grey to black vs. dashed grey to black lines). Thus, these changes modify the left-to-right gradients and may contribute to the perpetuation of arrhythmia. To account for variability in AP morphology between and within atria, we also varied K^+ and Ca^{2+} current densities (reduced I_{Kur} by 50%, increased I_{CaL} and I_{Kr} by 50% and 400% respectively) to produce a Type-1 AP, i.e., similar to the manipulation attempted in an earlier modeling study by Nygren and co-workers. [9] This results in a larger I_K and I_K/I_{to} ratio, more depolarized plateau potential, and steeper phase 3 repolarization (Figure 7B, left) as reported by the Nattel group [36] (Figure 7B, right). Importantly, as in experiments,[28,37] we show that when I_{Kur} is blocked Type-3 AP prolongs (7C, left), whereas Type-1 APD is almost unaltered (7C, right).

Discussion

We developed a new mathematical model of human atrial myocyte with detailed electrophysiology and Ca^{2+} handling, including ionic and Ca^{2+} handling remodeling in cAF.

This places our present understanding of atrial myocyte function in a useful quantitative framework to understand how changes in ion channel and Ca^{2+} handling influence function.

Atrial vs. ventricular cell models

Understanding atrio-ventricular ionic differences is important, has been investigated in simulations and experiments [38, 39], and may lead to safer therapy as a result of targeting atrial-specific ion channels for AF [1, 40]. We used the Grandi-Pasqualini-Bers model of the human ventricular AP and CaT [12] as a framework for model development. As a result, the two models have a common format and similar aspects that may be convenient for integrating into whole heart models. Similarities include the Ca^{2+} handling processes, which is also based on the Shannon-Bers model of the rabbit ventricular myocyte [41]. However, appropriate changes to many model parameters were introduced to recapitulate experimental findings in atrial samples from patients in sinus rhythm and cAF. Specific amalgams of ion channel expression and function confers differential AP characteristics for various cardiac regions [42, 43]. For example, it is well known that atrial I_{K1} density is smaller than ventricular I_{K1}, explaining the slightly less negative atrial diastolic membrane potential (by ~5 to 10 mV), reduced Na^+ channel availability and slower phase-3 repolarization [43]. Again, in humans, I_{Kur} is present in atria but not in ventricles [44], and in human atrium, I_{to} is encoded entirely by Kv4.3 (responsible for $I_{to,fast}$) [45], whereas both fast and slow I_{to} components are detected in human ventricle. We also simulated different AP morphologies and included right-to-left gradients in I_{to} and I_{Kur} as reported recently in human myocytes from the RA and the LA from patients in sinus rhythm or with cAF. This new set of models accounting for tissue-specific ion current differences will be useful for understanding regional electrophysiology, Ca^{2+} handling and arrhythmia mechanisms.

Novelties of the model compared to previous models

Computational cell modeling has been widely used to understand how individual ionic/molecular components (often studied in isolation) interact in the integrated environment of the cardiac myocyte. For human atrial myocyte models, the Courtemanche [10] and Nygren [9] models, which focused primarily on ion channels generating the atrial AP, have been useful to investigate physiological [46, 47] and pathophysiological [48, 49] mechanisms of the human atrium. However, those models have vastly different properties, especially in their rate-dependent behavior [50]. Recently, Maleckar *et al*. [8] incorporated new experimental K^+ current data into the Nygren model, including formulations of I_{Kur} and I_{to} that we have also adopted here. They also studied the early and late phase of atrial repolarization and improved the rate-dependent properties of the AP model.

However, no previous model focused on Ca^{2+} handling properties of human atrial myocytes, and it is increasingly clear that Ca^{2+}-handling and electrophysiology are intimately linked with respect to arrhythmias[7]. Cherry *et al*. [50] showed CaT differences between the two above models, with a more gradual longer lasting transient in the Courtemanche compared to a much sharper CaT in the Nygren/Maleckar models. Our human model uses the Ca^{2+} handling framework developed by Shannon *et al*. for rabbit ventricular myocytes [41], which was the first to introduce both a junctional cleft (where ryanodine receptor, RyR, and most I_{CaL} function) and also a subsarcolemmal Ca^{2+} compartment, where Ca^{2+}-dependent currents (e.g. I_{NCX} and $I_{Cl(Ca)}$) sense different local $[Ca^{2+}]_i$ compared to bulk $[Ca^{2+}]_i$ [51]. We have characterized Ca^{2+} handling properties in atrial myocytes from patients in sinus rhythm and with cAF, and modified the Ca^{2+} handling parameters in our model accordingly. This recapitulates experimental data including simultaneous measurements of I_{CaL} and CaT, caffeine-induced CaT amplitude (i.e., SR content) and decay time (i.e., SERCA and NCX function) and SR Ca^{2+} leak at physiological temperature. Our human atrial model provides an accurate representation of Ca^{2+} homeostasis in human atrial myocytes.

Recently, the Tavi group proposed a model describing heterogeneous subcellular Ca^{2+} dynamics for human atrial cells presumed to lack of t-tubules.[11] They produced a biphasic rise of $[Ca^{2+}]_i$, as seen at 22°C in human atrial myocytes.[52] In their model the biphasic $[Ca^{2+}]_i$ rise resulted from delay between peripheral and central SR Ca^{2+} release. An extensive t-tubular network has been reported in atrial myocytes from large mammals.[53] Because we did not observe biphasic $[Ca^{2+}]_i$ rise in our human atrial myocytes at 37°C (time to peak ~60 ms) and quantitative data on t-tubule organization in human atrial myocytes is lacking, we did not assume slow propagating Ca^{2+} release toward the cell center.

Rate-dependent APD adaptation

Using our human ventricular myocyte model, we found that the increase in $[Na^+]_i$ at fast pacing rates feeds back to shorten APD via outward (repolarizing) shifts in Na^+/K^+ pump (NKA) and NCX currents[12]. Our human atrial model (Figure 5) and that of the Tavi group[11] exhibit analogous behavior. The model showed negligible APD-rate adaptation when $[Na^+]_i$ was clamped to a certain value (Figure 5A). Notably, we confirmed experimentally in human atrial myocytes the prediction of our model that acutely blocking NKA causes AP prolongation followed by APD shortening (Figure 5C and D), thus supporting the involvement of $[Na^+]_i$ in APD (via shift in NKA current, Fig. 5B) and rate-dependent APD adaptation in human atrial cells. Furthermore, we show that I_{CaL} block has a similar effect on normal (sinus rhythm) and cAF human atrial action potentials (Figure 4), and in fact similar reductions in APD and APD rate-dependence occur in atrial myocytes isolated from patients with chronic AF. If I_{CaL} is blocked, APD is shorter (less depolarizing current), but also the CaT is greatly diminished, causing less extrusion of Ca^{2+} and less Na^+ entry via NCX. In addition, the positive inotropy observed in normal atrial myocytes is lost in cAF, also limiting NCX-dependent Na^+ accumulation at fast rates (as in Fig. 3I). Thus, our model recapitulated experimental results and point to $[Na^+]_i$ and I_{CaL} as critical components of the normal rate–dependent modulation of atrial APD. While direct effects of $[Na^+]_i$ on APD are compelling and logical, additional experimental validation of these effect would be valuable. We have discussed previously the role of delayed-rectifier K^+ currents in APD rate adaptation [12], and showed in Online Figure VII that I_{Kr} block has little effect on APD. Here we ruled out an important role of the atrial-predominant I_{Kur} (see Online Figure VIII).

Role of $[Ca^{2+}]_i$ in mediating AF in presence of I_{Kur} channelopathies

Atrial contractility is decreased in cAF, largely due to electrical remodeling that is associated with downregulation of I_{CaL} [28, 29], which reduces CaT amplitude. Our simulation demonstrated that block of I_{Kur} enhances CaT amplitude of human atrial myocytes, both in patients in sinus rhythm or AF (Figure 6), thus pointing to I_{Kur} as an atrial-specific target to counteract hypocontractility associated to cAF. Indeed, experiments have shown that I_{Kur} blockers in ventricle did not appreciably alter APD or CaT [29].

We hypothesize that I_{Kur} in the atrium may serve the same function as I_{Ks} in the ventricle, that is opposing AP prolongation expected from larger inward I_{CaL} and I_{NCX} during β-adrenergic stress [54]. Indeed, our simulations showed that block of I_{Kur} (to mimic Kv1.5 mutation that leads to non-functional current, and AF) in the presence of adrenergic challenge causes EADs (Figure 6D). That agrees with experimental data[14], where I_{Kur} inhibition led to EADs in human atrial myocytes challenged with ISO. On the other hand, I_{Ks} block did not appreciably affect APD. Administration of ISO also led to cellular arrhythmic depolarizations when stimulating our model at low pacing frequency (not shown), in accordance with experimental work [14, 55].

Conclusions

We developed a new computational framework to study the contribution of individual ionic pathway differences between atrial and ventricular cells to AP phenotype difference in the human atrium vs. ventricle. It also established that Ca^{2+} and Na^{+} handling processes are major contributors to atrial APD and its rate-related behavior in both normal and cAF conditions, and identified the role of I_{Kur} in helping prevent EADs in the presence of adrenergic stress. This model (freely available at https://somapp.ucdmc.ucdavis.edu/Pharmacology/bers/) will also be useful for integrating into multicellular models of the human heart.

Supplementary Material

Refer to Web version on PubMed Central for supplementary material.

Acknowledgments

Authors thank the Heidelberg Cardiosurgeon Team for the provision of human atrial tissue and Claudia Liebetrau and Katrin Kupser for excellent technical assistance. Authors also thank the cardiothoracic surgical team, Golden Jubilee National Hospital, Glasgow, UK, for provision of human atrial tissue.

Sources of Funding NHLBI Grants P01-HL080101 and R37-HL30077 (DMB), P01-HL039707, P01-HL070074 and R01-HL080159 (JJ); AHA Scientist Development Grant (SVP); British Heart Foundation Basic Science Lectureship BS/06/003 (AJW); Fondation Leducq Transatlantic Alliances for Atrial Fibrillation (DD) and CaMKII (DMB).

References

1. Benjamin EJ, Chen PS, Bild DE, Mascette AM, Albert CM, Alonso A, Calkins H, Connolly SJ, Curtis AB, Darbar D, Ellinor PT, Go AS, Goldschlager NF, Heckbert SR, Jalife J, Kerr CR, Levy D, Lloyd-Jones DM, Massie BM, Nattel S, Olgin JE, Packer DL, Po SS, Tsang TS, Van Wagoner DR, Waldo AL, Wyse DG. Prevention of atrial fibrillation: report from a national heart, lung, and blood institute workshop. Circulation. 2009; 119(4):606–618. [PubMed: 19188521]
2. Jalife J. Deja vu in the theories of atrial fibrillation dynamics. Cardiovasc Res. 2011; 89(4):766–775. [PubMed: 21097807]
3. Nattel S, Burstein B, Dobrev D. Atrial Remodeling and Atrial Fibrillation. Circulation: Arrhythmia and Electrophysiology. 2008; 1(1):62–73. [PubMed: 19808395]
4. Dobrev D, Ravens U. Remodeling of cardiomyocyte ion channels in human atrial fibrillation. Basic Res Cardiol. 2003; 98:137–148. [PubMed: 12883831]
5. Workman AJ, Kane KA, Rankin AC. Cellular bases for human atrial fibrillation. Heart Rhythm. 2008; 5(6 Suppl):S1–6. [PubMed: 18456193]
6. Dobrev D, Nattel S. Calcium Handling Abnormalities in Atrial Fibrillation as a Target for Innovative Therapeutics. Journal of Cardiovascular Pharmacology. 2008; 52(4):293–299. [PubMed: 18791467]
7. Dobrev D, Voigt N, Wehrens XHT. The ryanodine receptor channel as a molecular motif in atrial fibrillation: pathophysiological and therapeutic implications. Cardiovascular Research. 2011; 89(4): 734–743. [PubMed: 20943673]
8. Maleckar MM, Greenstein JL, Giles WR, Trayanova NA. K^{+} current changes account for the rate dependence of the action potential in the human atrial myocyte. Am J Physiol Heart Circ Physiol. 2009; 297(4):H1398–1410. [PubMed: 19633207]
9. Nygren A, Fiset C, Firek L, Clark JW, Lindblad DS, Clark RB, Giles WR. Mathematical Model of an Adult Human Atrial Cell : The Role of K^{+} Currents in Repolarization. Circ Res. 1998; 82(1):63–81. [PubMed: 9440706]
10. Courtemanche M, Ramirez RJ, Nattel S. Ionic mechanisms underlying human atrial action potential properties: insights from a mathematical model. Am J Physiol Heart Circ Physiol. 1998; 275(1):H301–321.

11. Koivumaki JT, Korhonen T, Tavi P. Impact of sarcoplasmic reticulum calcium release on calcium dynamics and action potential morphology in human atrial myocytes: a computational study. PLoS Comput Biol. 2011; 7(1):e1001067. [PubMed: 21298076]
12. Grandi E, Pasqualini FS, Bers DM. A novel computational model of the human ventricular action potential and Ca transient. Journal of Molecular and Cellular Cardiology. 2010; 48(1):112–121. [PubMed: 19835882]
13. Hatem SN, Coulombe A, Balse E. Specificities of atrial electrophysiology: Clues to a better understanding of cardiac function and the mechanisms of arrhythmias. J Mol Cell Cardiol. 2010; 48(1):90–95. [PubMed: 19744488]
14. Olson TM, Alekseev AE, Liu XK, Park S, Zingman LV, Bienengraeber M, Sattiraju S, Ballew JD, Jahangir A, Terzic A. Kv1.5 channelopathy due to KCNA5 loss-of-function mutation causes human atrial fibrillation. Hum Mol Genet. 2006; 15(14):2185–2191. [PubMed: 16772329]
15. Dawodu AA, Monti F, Iwashiro K, Schiariti M, Chiavarelli R, Puddu PE. The shape of human atrial action potential accounts for different frequency-related changes in vitro. Int J Cardiol. 1996; 54(3):237–249. [PubMed: 8818747]
16. Workman AJ, Kane KA, Rankin AC. The contribution of ionic currents to changes in refractoriness of human atrial myocytes associated with chronic atrial fibrillation. Cardiovascular Research. 2001; 52(2):226–235. [PubMed: 11684070]
17. Voigt N, Trafford AW, Ravens U, Dobrev D. Abstract 2630: Cellular and Molecular Determinants of Altered Atrial Ca^{2+} Signaling in Patients With Chronic Atrial Fibrillation. Circulation. 2009; 120:S667–d-668. 18_MeetingAbstracts.
18. Christ T, Boknik P, Wohrl S, Wettwer E, Graf EM, Bosch RF, Knaut M, Schmitz W, Ravens U, Dobrev D. L-Type Ca^{2+} Current Downregulation in Chronic Human Atrial Fibrillation Is Associated With Increased Activity of Protein Phosphatases. Circulation. 2004; 110(17):2651–2657. [PubMed: 15492323]
19. Van Wagoner DR, Pond AL, Lamorgese M, Rossie SS, McCarthy PM, Nerbonne JM. Atrial L-Type Ca^{2+} Currents and Human Atrial Fibrillation. Circ Res. 1999; 85(5):428–436. [PubMed: 10473672]
20. Li GR, Nattel S. Properties of human atrial I_{Ca} at physiological temperatures and relevance to action potential. Am J Physiol Heart Circ Physiol. 1997; 272(1):H227–235.
21. Dobrev D, Graf E, Wettwer E, Himmel HM, Hala O, Doerfel C, Christ T, Schuler S, Ravens U. Molecular Basis of Downregulation of G-Protein-Coupled Inward Rectifying K^+ Current ($I_{K,ACh}$) in Chronic Human Atrial Fibrillation: Decrease in GIRK4 mRNA Correlates With Reduced $I_{K,ACh}$ and Muscarinic Receptor-Mediated Shortening of Action Potentials. Circulation. 2001; 104(21):2551–2557. [PubMed: 11714649]
22. Boutjdir M, Le Heuzey J, Lavergne T, Chauvaud S, Guize L, Carpentier A, Peronneau P. Inhomogeneity of cellular refractoriness in human atrium: factor of arrhythmia? Pacing Clin Electrophysiol. 1986; 9(6 Pt 2):1095–1100. [PubMed: 2432515]
23. Bosch RF, Zeng X, Grammer JB, Popovic K, Mewis C, Kuhlkamp V. Ionic mechanisms of electrical remodeling in human atrial fibrillation. Cardiovasc Res. 1999; 44(1):121–131. [PubMed: 10615396]
24. Maier LS, Barckhausen P, Weisser J, Aleksic I, Baryalei M, Pieske B. Ca^{2+} handling in isolated human atrial myocardium. Am J Physiol Heart Circ Physiol. 2000; 279(3):H952–958. [PubMed: 10993755]
25. Schotten U, Greiser M, Benke D, Buerkel K, Ehrenteidt B, Stellbrink C, Vazquez-Jimenez JF, Schoendube F, Hanrath P, Allessie M. Atrial fibrillation-induced atrial contractile dysfunction: a tachycardiomyopathy of a different sort. Cardiovasc Res. 2002; 53(1):192–201. [PubMed: 11744028]
26. Rocchetti M, Besana A, Mostacciuolo G, Ferrari P, Micheletti R, Zaza A. Diverse toxicity associated with cardiac Na^+/K^+ pump inhibition: evaluation of electrophysiological mechanisms. J Pharmacol Exp Ther. 2003; 305(2):765–771. [PubMed: 12606646]
27. Hordof AJ, Spotnitz A, Mary-Rabine L, Edie RN, Rosen MR. The cellular electrophysiologic effects of digitalis on human atrial fibers. Circulation. 1978; 57(2):223–229. [PubMed: 618608]

28. Wettwer E, Hala O, Christ T, Heubach JF, Dobrev D, Knaut M, Varro A, Ravens U. Role of I_{Kur} in controlling action potential shape and contractility in the human atrium: influence of chronic atrial fibrillation. Circulation. 2004; 110(16):2299–2306. [PubMed: 15477405]
29. Schotten U, de Haan S, Verheule S, Harks EG, Frechen D, Bodewig E, Greiser M, Ram R, Maessen J, Kelm M, Allessie M, Van Wagoner DR. Blockade of atrial-specific K^+-currents increases atrial but not ventricular contractility by enhancing reverse mode Na^+/Ca^{2+}-exchange. Cardiovasc Res. 2007; 73(1):37–47. [PubMed: 17157284]
30. Workman AJ. Cardiac adrenergic control and atrial fibrillation. Naunyn Schmiedebergs Arch Pharmacol. 2010; 381(3):235–249. [PubMed: 19960186]
31. Soltis AR, Saucerman JJ. Synergy between CaMKII substrates and beta-adrenergic signaling in regulation of cardiac myocyte Ca^{2+} handling. Biophys J. 2010; 99(7):2038–2047. [PubMed: 20923637]
32. Heijman J, Volders PG, Westra RL, Rudy Y. Local control of beta-adrenergic stimulation: Effects on ventricular myocyte electrophysiology and Ca^{2+}-transient. J Mol Cell Cardiol. 2011; 50(5): 863–871. [PubMed: 21345340]
33. Caballero R, de la Fuente MG, Gómez R, Barana A, Amorós I, Dolz-Gaitón P, Osuna L, Almendral J, Atienza F, Fernández-Avilés F, Pita A, Rodríguez-Roda J, Pinto Á, Tamargo J, Delpón E. In Humans, Chronic Atrial Fibrillation Decreases the Transient Outward Current and Ultrarapid Component of the Delayed Rectifier Current Differentially on Each Atria and Increases the Slow Component of the Delayed Rectifier Current in Both. Journal of the American College of Cardiology. 2010; 55(21):2346–2354. [PubMed: 20488306]
34. Voigt N, Trausch A, Knaut M, Matschke K, Varro A, Van Wagoner DR, Nattel S, Ravens U, Dobrev D. Left-to-right atrial inward rectifier potassium current gradients in patients with paroxysmal versus chronic atrial fibrillation. Circ Arrhythm Electrophysiol. 2010; 3(5):472–480. [PubMed: 20657029]
35. Narayan SM, Kazi D, Krummen DE, Rappel WJ. Repolarization and activation restitution near human pulmonary veins and atrial fibrillation initiation: a mechanism for the initiation of atrial fibrillation by premature beats. J Am Coll Cardiol. 2008; 52(15):1222–1230. [PubMed: 18926325]
36. Wang Z, Fermini B, Nattel S. Delayed rectifier outward current and repolarization in human atrial myocytes. Circ Res. 1993; 73(2):276–285. [PubMed: 8330373]
37. Firek L, Giles WR. Outward currents underlying repolarization in human atrial myocytes. Cardiovasc Res. 1995; 30(1):31–38. [PubMed: 7553721]
38. Pandit SV, Berenfeld O, Anumonwo JM, Zaritski RM, Kneller J, Nattel S, Jalife J. Ionic determinants of functional reentry in a 2-D model of human atrial cells during simulated chronic atrial fibrillation. Biophys J. 2005; 88(6):3806–3821. [PubMed: 15792974]
39. Pandit SV, Zlochiver S, Filgueiras-Rama D, Mironov S, Yamazaki M, Ennis SR, Noujaim SF, Workman AJ, Berenfeld O, Kalifa J, Jalife J. Targeting atrioventricular differences in ion channel properties for terminating acute atrial fibrillation in pigs. Cardiovasc Res. 2011; 89(4):843–851. [PubMed: 21076156]
40. Dobrev D, Nattel S. New antiarrhythmic drugs for treatment of atrial fibrillation. The Lancet. 2010; 375(9721):1212–1223.
41. Shannon TR, Wang F, Puglisi J, Weber C, Bers DM. A Mathematical Treatment of Integrated Ca Dynamics within the Ventricular Myocyte. Biophys J. 2004; 87(5):3351–3371. [PubMed: 15347581]
42. Gaborit N, Le Bouter S, Szuts V, Varro A, Escande D, Nattel S, Demolombe S. Regional and tissue specific transcript signatures of ion channel genes in the non-diseased human heart. The Journal of Physiology. 2007; 582(2):675–693. [PubMed: 17478540]
43. Schram G, Pourrier M, Melnyk P, Nattel S. Differential Distribution of Cardiac Ion Channel Expression as a Basis for Regional Specialization in Electrical Function. Circ Res. 2002; 90(9): 939–950. [PubMed: 12016259]
44. Li G-R, Feng J, Yue L, Carrier M, Nattel S. Evidence for Two Components of Delayed Rectifier K^+ Current in Human Ventricular Myocytes. Circ Res. 1996; 78(4):689–696. [PubMed: 8635226]

45. Wang Z, Feng J, Shi H, Pond A, Nerbonne JM, Nattel S. Potential Molecular Basis of Different Physiological Properties of the Transient Outward K^+ Current in Rabbit and Human Atrial Myocytes. Circ Res. 1999; 84(5):551–561. [PubMed: 10082477]
46. Severi S, Corsi C, Cerbai E. From in vivo plasma composition to in vitro cardiac electrophysiology and in silico virtual heart: the extracellular calcium enigma. Philosophical Transactions of the Royal Society A: Mathematical, Physical and Engineering Sciences. 2009; 367(1896):2203–2223.
47. Tsujimae K, Suzuki S, Murakami S, Kurachi Y. Frequency-dependent effects of various I_{Kr} blockers on cardiac action potential duration in a human atrial model. American Journal of Physiology - Heart and Circulatory Physiology. 2007; 293(1):H660–H669. [PubMed: 17220183]
48. Zhang H, Garratt CJ, Zhu J, Holden AV. Role of up-regulation of I_{K1} in action potential shortening associated with atrial fibrillation in humans. Cardiovascular Research. 2005; 66(3): 493–502. [PubMed: 15914114]
49. Courtemanche M, Ramirez RJ, Nattel S. Ionic targets for drug therapy and atrial fibrillation-induced electrical remodeling: insights from a mathematical model. Cardiovascular Research. 1999; 42(2):477–489. [PubMed: 10533583]
50. Cherry EM, Hastings HM, Evans SJ. Dynamics of human atrial cell models: Restitution, memory, and intracellular calcium dynamics in single cells. Progress in Biophysics and Molecular Biology. 2008; 98(1):24–37. [PubMed: 18617227]
51. Weber CR, Piacentino V III, Ginsburg KS, Houser SR, Bers DM. Na^+-Ca^{2+} Exchange Current and Submembrane [Ca^{2+}] During the Cardiac Action Potential. Circ Res. 2002; 90(2):182–189. [PubMed: 11834711]
52. Hatem SN, Benardeau A, Rucker-Martin C, Marty I, de Chamisso P, Villaz M, Mercadier JJ. Different compartments of sarcoplasmic reticulum participate in the excitation-contraction coupling process in human atrial myocytes. Circ Res. 1997; 80(3):345–353. [PubMed: 9048654]
53. Lenaerts I, Bito V, Heinzel FR, Driesen RB, Holemans P, D'Hooge J, Heidbuchel H, Sipido KR, Willems R. Ultrastructural and Functional Remodeling of the Coupling Between Ca^{2+} Influx and Sarcoplasmic Reticulum Ca^{2+} Release in Right Atrial Myocytes From Experimental Persistent Atrial Fibrillation. Circ Res. 2009; 105(9):876–885. [PubMed: 19762679]
54. Jost N, Virag L, Bitay M, Takacs J, Lengyel C, Biliczki P, Nagy Z, Bogats G, Lathrop DA, Papp JG, Varro A. Restricting excessive cardiac action potential and QT prolongation: a vital role for I_{Ks} in human ventricular muscle. Circulation. 2005; 112(10):1392–1399. [PubMed: 16129791]
55. Redpath CJ, Rankin AC, Kane KA, Workman AJ. Anti-adrenergic effects of endothelin on human atrial action potentials are potentially anti-arrhythmic. J Mol Cell Cardiol. 2006; 40(5):717–724. [PubMed: 16603181]
56. Sossalla S, Kallmeyer B, Wagner S, Mazur M, Maurer U, Toischer K, Schmitto JD, Seipelt R, Schondube FA, Hasenfuss G, Belardinelli L, Maier LS. Altered Na^+ currents in atrial fibrillation effects of ranolazine on arrhythmias and contractility in human atrial myocardium. J Am Coll Cardiol. 2010; 55(21):2330–2342. [PubMed: 20488304]
57. Shannon TR, Wang F, Bers DM. Regulation of Cardiac Sarcoplasmic Reticulum Ca Release by Luminal [Ca] and Altered Gating Assessed with a Mathematical Model. Biophysical Journal. 2005; 89(6):4096–4110. [PubMed: 16169970]
58. Li G-R, Feng J, Wang Z, Fermini B, Nattel S. Adrenergic Modulation of Ultrarapid Delayed Rectifier K^+ Current in Human Atrial Myocytes. Circ Res. 1996; 78(5):903–915. [PubMed: 8620611]
59. Amos GJ, Wettwer E, Metzger F, Li Q, Himmel HM, Ravens U. Differences between outward currents of human atrial and subepicardial ventricular myocytes. The Journal of Physiology. 1996; 491(Pt 1):31–50. [PubMed: 9011620]
60. Wang J, Schwinger RH, Frank K, Müller-Ehmsen J, Martin-Vasallo P, Pressley TA, Xiang A, Erdmann E, McDonough AA. Regional expression of sodium pump subunits isoforms and Na^+-Ca^{2+} exchanger in the human heart. The Journal of Clinical Investigation. 1996; 98(7):1650. [PubMed: 8833915]
61. Neef S, Dybkova N, Sossalla S, Ort KR, Fluschnik N, Neumann K, Seipelt R, Schondube FA, Hasenfuss G, Maier LS. CaMKII-Dependent Diastolic SR Ca^{2+} Leak and Elevated Diastolic Ca^{2+}

Levels in Right Atrial Myocardium of Patients With Atrial Fibrillation. Circ Res. 2010; 106(6): 1134–1144. [PubMed: 20056922]

62. El-Armouche A, Boknik P, Eschenhagen T, Carrier L, Knaut M, Ravens U, Dobrev D. Molecular determinants of altered Ca^{2+} handling in human chronic atrial fibrillation. Circulation. 2006; 114(7):670–680. [PubMed: 16894034]
63. Boknik P, Unkel C, Kirchhefer U, Kleideiter U, Klein-Wiele O, Knapp J, Linck B, Luss H, Ulrich Muller F, Schmitz W, Vahlensieck U, Zimmermann N, Jones LR, Neumann J. Regional expression of phospholamban in the human heart. Cardiovasc Res. 1999; 43(1):67–76. [PubMed: 10536691]
64. Workman AJ, Kane KA, Rankin AC. Characterisation of the Na, K pump current in atrial cells from patients with and without chronic atrial fibrillation. Cardiovasc Res. 2003; 59(3):593–602. [PubMed: 14499860]
65. Despa S, Bossuyt J, Han F, Ginsburg KS, Jia L-G, Kutchai H, Tucker AL, Bers DM. Phospholemman-Phosphorylation Mediates the {beta}-Adrenergic Effects on Na/K Pump Function in Cardiac Myocytes. Circ Res. 2005; 97(3):252–259. [PubMed: 16002746]

Non-standard Abbreviations and Acronyms

AF	Atrial Fibrillation
AP	Action Potential
APD	Action Potential Duration
APD_{90}	Action Potential Duration at 90% repolarization
cAF	chronic Atrial Fibrillation
CaT	Ca^{2+} transient
EAD	Early After Depolarization
G_{NaL}	Late Na^+ current maximal conductance
I_{CaL}	L-type Ca^{2+} current
$I_{Cl(Ca)}$	Ca^{2+}-activated Cl^- current
I_{KACh}	Acetylcholine-activated K^+ current
I_{Kr}	Rapidly activating delayed rectifier K^+ current
I_{Ks}	Slowly activating delayed rectifier K^+ current
I_{Kur}	Ultrarapid delayed rectifier K^+ current
I_{K1}	Inward rectifier K^+ current
I_{Na}	Fast Na^+ current
I_{NCX}	Na^+/Ca^{2+} exchange current
I_{NaK}	Na^+/K^+ pump current
ISO	Isoproterenol
I_{to}	Transient outward K^+ current
LA	Left Atrium
NCX	Na^+/Ca^{2+} exchange
NKA	Na^+/K^+ ATPase
PKA	Protein Kinase A

RA	Right Atrium
RyR	Ryanodine Receptor
SERCA	Sarcoplasmic Reticulum Ca^{2+} ATPase
SK2	Ca^{2+}-activated K^+ channels
sr	sinus rhythm
SR	Sarcoplasmic Reticulum

Novelty and Significance

What is Known?

- Atrial cells exhibit electrophysiological characteristics that differ from those of ventricular cells due to structural differences and specific combinations of ion channel/transporters expression and function.
- During chronic atrial fibrillation (AF), electrical and structural remodeling contributes to the development of the AF substrate, and abnormalities in intracellular Ca^{2+} cycling has emerged as key mediators in AF pathophysiology.
- Detailed models of myocyte Ca^{2+} cycling have typically focused on ventricular rather than atrial myocytes, in part because of limited appropriate experimental data (especially from human atrial myocytes).

What New Information Does This Article Contribute?

- Based on recent data from human atrial cells, we have developed a new mathematical model of the human atrial myocyte that accounts for the electrophysiological and Ca^{2+} handling properties of atrial cells in both normal and chronic AF conditions.
- Simulations indicate that heart rate-dependent action potential duration (APD) shortening in healthy atrial cells involves the accumulation of intracellular $[Na^+]$ at high frequencies that causes outward shifts in Na^+/Ca^{2+} exchange and Na^+/K^+ pump currents, whereas ionic and Ca^{2+} handling remodeling lead to reduced Na^+ accumulation in chronic AF, which causes a blunted APD rate-dependent response.
- Our modeling suggests that I_{Kur} is a key component of the adrenergic response of human atrial cells, as its loss (such as in Kv1.5 channelopathy) results in predisposition to early-afterdepolarizations in presence of isoproterenol, and may help explain the bouts of stress mediated AF observed in these patients.

It is increasingly clear that Ca^{2+}-handling and electrophysiology are intimately linked to the development and perpetuation of AF. Thus, understanding AF requires an integrated quantitative understanding of ionic currents and Ca^{2+} transport in healthy and remodeled human atrium. However, no previous model focused on Ca^{2+} transport in human atrial myocytes in chronic AF. We developed a new human atrial myocyte model that incorporates the latest experimental data and modern concepts relating to intracellular Ca^{2+} homeostasis and related electrophysiology, including ionic and Ca^{2+} handling remodeling seen in chronic AF. Our simulation showed that I_{Kur} block enhances the amplitude of the Ca^{2+} transient of human atrial myocytes, representing an atrial-specific target to counteract hypocontractility associated to cAF. This current is also predicted to oppose APD prolongation expected from larger inward I_{CaL} and I_{NCX} during β-adrenergic stress. Our model provides novel insights into the mechanism of APD rate-dependent adaptation, by showing that accumulation of $[Na^+]_i$ at fast heart rates feeds back to shorten APD via outward shifts in Na^+/Ca^{2+} exchange and Na^+/K^+ pump currents. This human atrial model provides a useful tool to investigate atrio-ventricular differences with respect to arrhythmogenesis and therapeutical approaches.

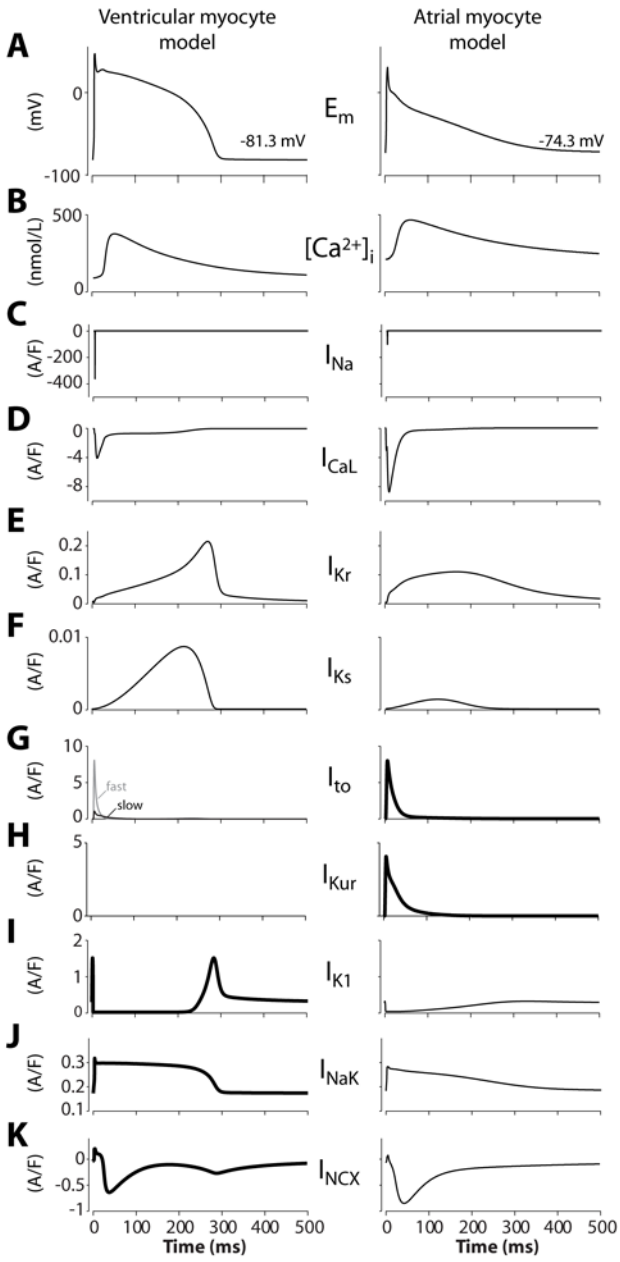

Figure 1.

Steady-state human cardiac AP and major underlying currents and CaT at 1 Hz pacing (**A-K**) for ventricle (left) and atrium (right). Thicker traces represent currents for which density was increased (in atria vs. ventricle or vice versa) because of altered maximal conductance or pump rate to generate the atrial cell model from the ventricular cell model.

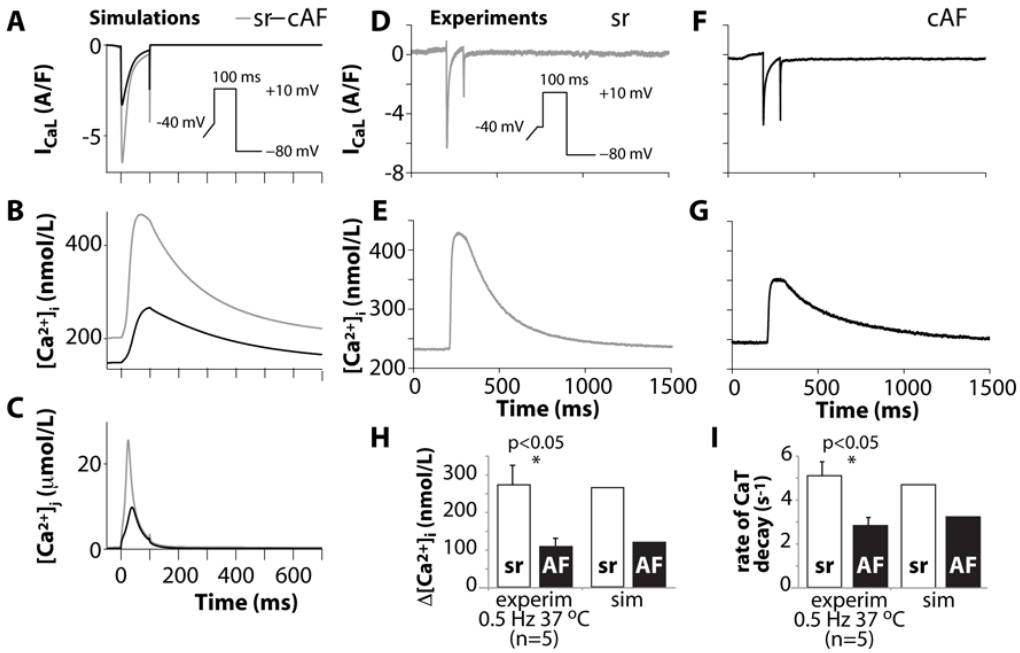

Figure 2.

Ca^{2+} current (**A**) and transient (**B**) were simulated for a voltage clamp protocol (A, *inset*) where membrane potential was stepped to +10 mV for 100 ms after a 100 ms duration ramp to -40mV to inactivate fast I_{Na} from a holding potential of -80 mV (pacing at 0.5 Hz). For cAF Ca^{2+} current amplitude is small compared to sinus rhythm (**A**, grey vs. black traces), as in experiments at physiological temperature in human atrial cells (**D** vs. **F**, protocol in **D**, *inset*). This leads to a strong reduction in CaT amplitude (**B** and **H**), also observed experimentally (**E** vs. **G, H**), which also limits the increase in junctional $[Ca^{2+}]$ (**C**). Twitch $[Ca^{2+}]_i$ decline rate (indicative of SERCA function) is slowed in cAF, in agreement with experiments (**I**).

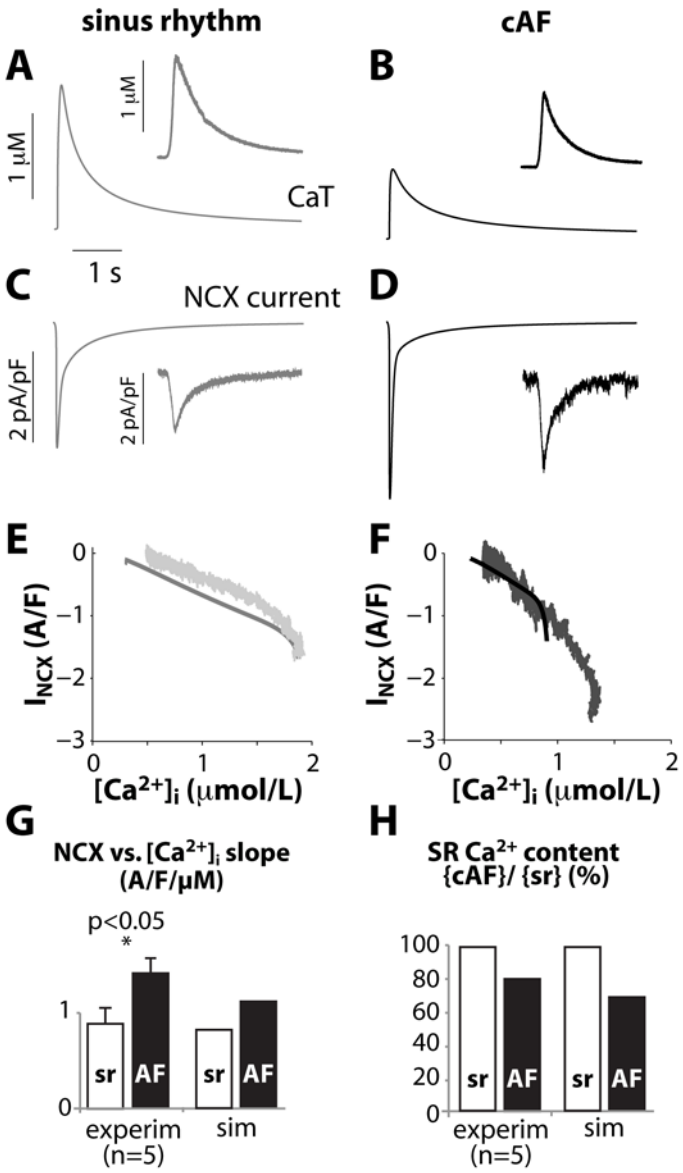

Figure 3.

Caffeine-induced CaT and I_{NCX} in sinus rhythm (**A** and **C**) and cAF (**B** and **D**) reveal a smaller SR Ca^{2+} content in cAF compared to sinus rhythm (**H**). The slope of NCX current vs. $[Ca^{2+}]_i$ during the decaying phase of the caffeine-evoked CaT (**E-F**) was higher in cAF vs. sinus rhythm (**G**).

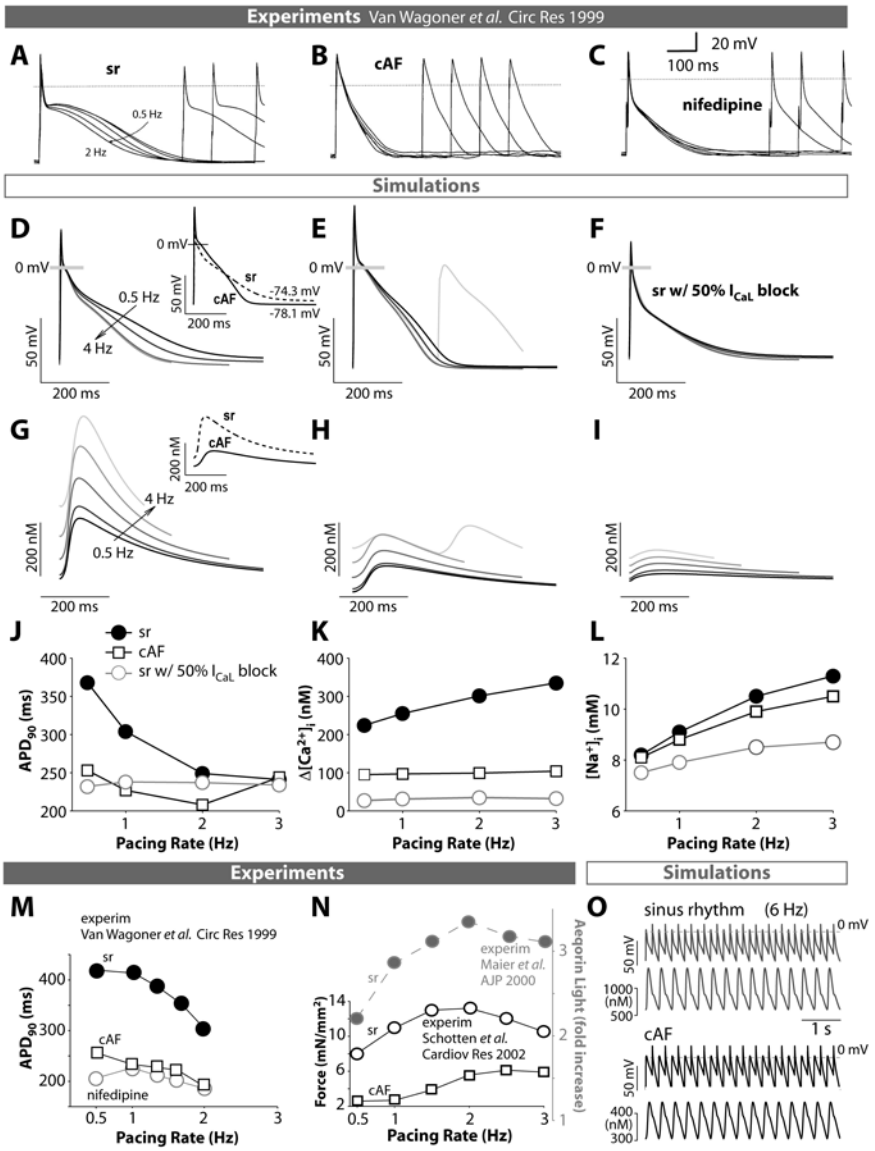

Figure 4.

APs recorded at different cycle lengths in a control human atrial myocyte (**A**), in a cell from cAF patient (**B**), and in the same control myocyte exposed to Ca^{2+} channel block (10 μmol/L nifedipine, **C**). [19] Simulated steady-state AP and CaT traces are shown for pacing frequencies 0.5, 1, 2, 3, and 4 Hz, for sinus rhythm (sr, **D** and **G**), cAF (**E** and **H**), and sr with 50% I_{CaL} block (**F** and **I**). Simulated APD_{90} (**J**) decreases at increasing pacing frequency in sr, but rate-adaptation is impaired in cAF or with I_{CaL} partially inhibited. Experimental results [19] are also reported (**M**). Predicted CaT amplitude (**K**) and $[Na^+]_i$ (**L**) increase with frequency in sr cells, in agreement with changes in aequorin signals in human atrial muscle strips (**N**, grey circles). Frequency-dependence of $[Ca^{2+}]_i$, $[Na^+]_i$ and force is limited in cAF or when I_{CaL} is partially inhibited (**K,L,N**). Alternating long and short APs and CaTs (**O**) are predicted in sr and cAF cells paced at 6 Hz.

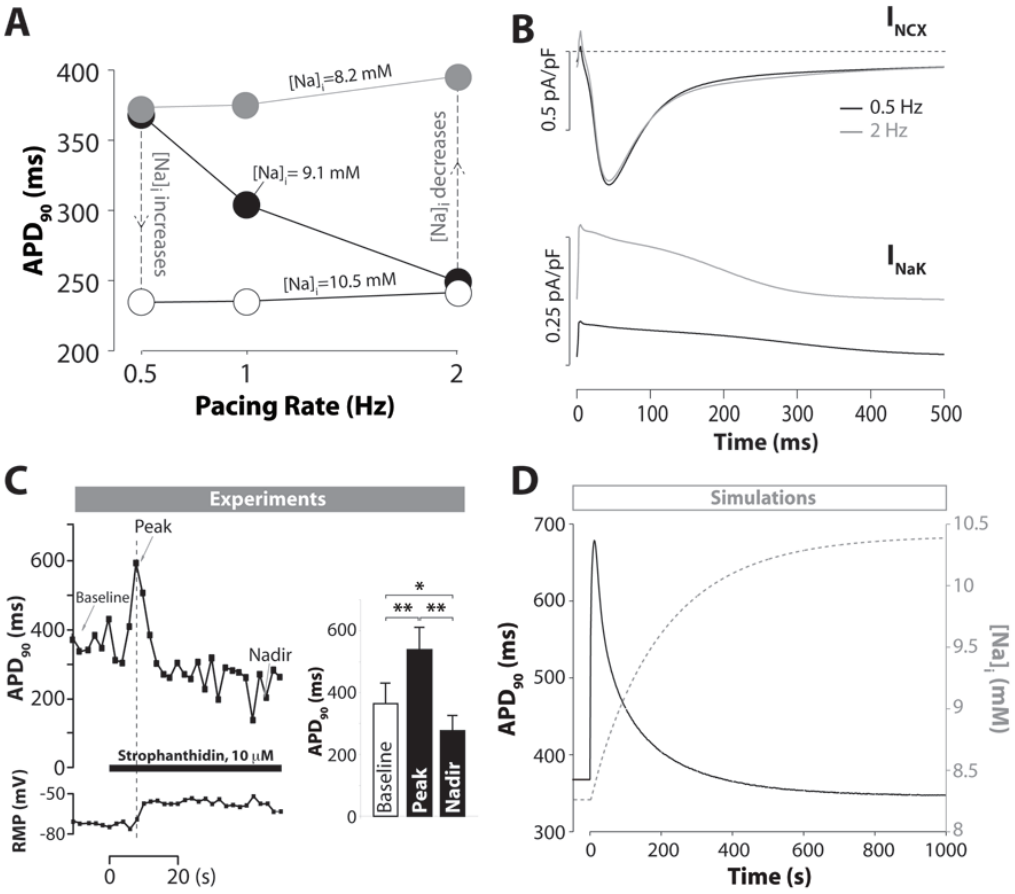

Figure 5.

A) APD_{90} decreases with increasing pacing frequency from 0.5 to 2 Hz and $[Na^+]_i$ changes freely (black circles). If the atrial myocyte is paced at low frequency, but with $[Na^+]_i$ clamped at 10.5 mmol/L (level predicted at fast rate), APD_{90} shortens (white circles) to APD_{90} value at 2 Hz. Similarly, when the atrial myocyte is paced at fast rate and $[Na^+]_i$ is clamped to the low level predicted with slow pacing, APD_{90} lengthens (gray circles) to APD_{90} value at 0.5 Hz. **B**) NKA and NCX currents at 0.5 and 2 Hz pacing rate. Experimental and simulated time courses of APD_{90} (**C** and **D**), resting membrane potential (**C**) and $[Na^+]_i$ (**D**) following application of strophanthidin (**C**) and partial (50%) I_{NaK} block (**D**, at time 0) at 0.5 Hz pacing rate. Effect of strophanthidin on mean APD_{90} (**C**, right). $p<0.05$ and $^{**}p<0.001$ with paired t-test and Bonferroni correction (n = 10 myocytes from 5 patients).

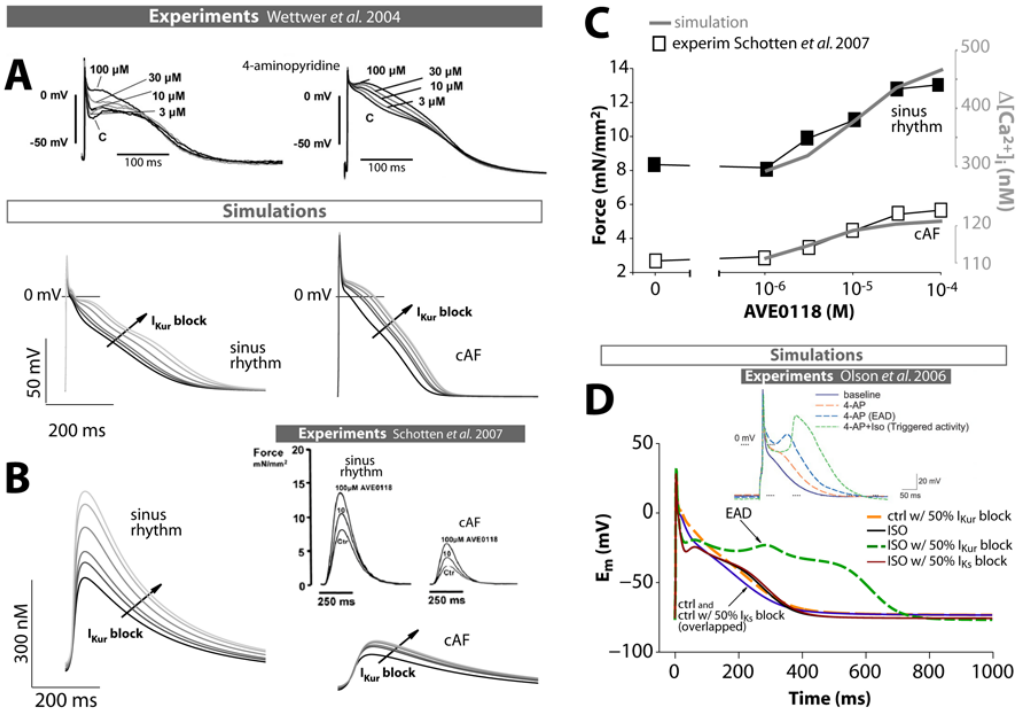

Figure 6.

Effect of different degrees of I_{Kur} block on simulated human atrial APD (**A**) and CaT (**B-C**) in sr and cAF is compared with experimental AP recordings [28] (**A**, *inset*) and twitch force measurements [29] (**B** *inset* and **C**). **D**) ISO application causes EADs (green dashed line) in the presence of I_{Kur} blockade, as shown experimentally by Olson *et al*. (**D**, *inset*) [14]. Blocking I_{Ks} does not have the same deleterious effect (red solid line).

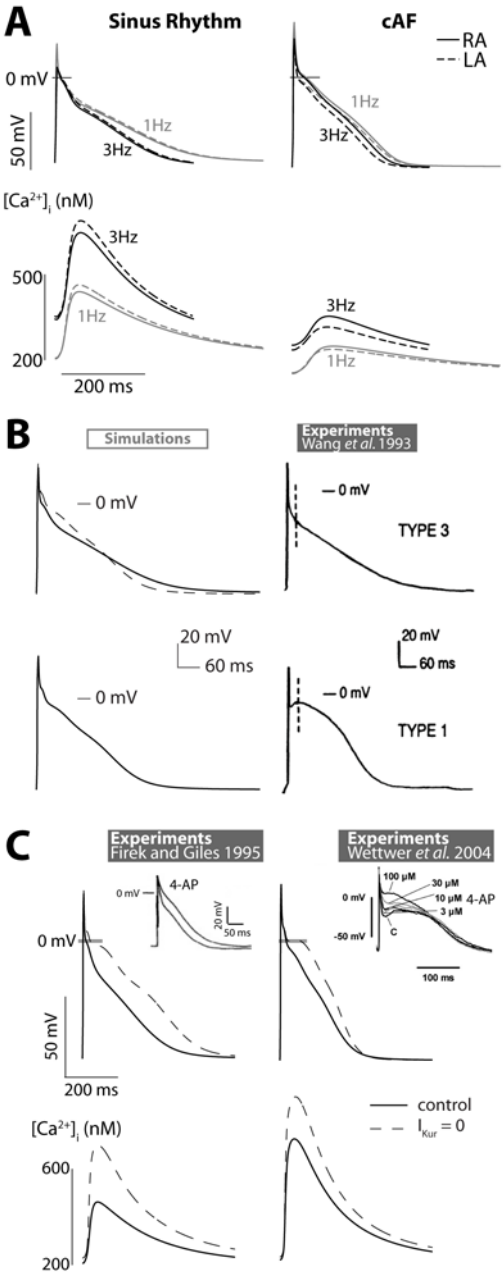

Figure 7.

A) Simulated APs and CaTs from right and left atria (RA and LA) at 1Hz and 3 Hz are shown in sinus rhythm (left) and cAF (right). **B**) Type-1 AP (dashed and bottom panel) was obtained by modifying K^+ and Ca^{2+} current densities in the nominal Type-3 AP (top panel, solid line). **C**) I_{Kur} block prolongs Type-3 APs (left) but has little effect on APD_{90} of Type-1 APs (right), as shown experimentally (*insets*) [28, 37]. CaTs are shown in bottom panels.

Table 1

Main changes to our human ventricular model to generate the human atrial model, simulate cAF, and β-adrenergic stimulation.

	Atrial vs. Ventricular	cAF vs. Sinus Rhythm	Adrenergic Stimulation
Ionic Currents			
I_{Na}	Unchanged	-10% peak density [56]	Unchanged
I_{NaL}	None	Added late component [56]	Unchanged
I_{Ks}	Unchanged	Increased 2-fold [33]	Enhanced maximal conductance (3 fold) and leftward shift in IV relationship (by 40 mV) [57]
I_{Kr}	Unchanged	Unchanged	Unchanged
I_{Kur}	Added	-55% in the RA -45% in the LA [4, 33]	Enhanced maximal conductance (3 fold) [58]
I_{K1}	85% reduction [43]	Upregulated +100% [4, 21]	Unchanged
I_{to}	No $I_{to,slow}$ $I_{to,fast}$: activation and inactivation negatively shifted and slower inactivation; larger amplitude [59]	$I_{to,fast}$ -80% in the RA -45% in the LA[4, 33]	Unchanged
Ca and Na handling			
I_{CaL}	Matched amplitude and kinetics at 37°C from our data and [20]	Current density is reduced by 50% in cAF [4, 17, 18] (and present data) No changes in voltage dependence of activation and inactivation [19]	Increased fraction of available channels (+50%), and channel availability shifted leftward (by 3mV) [57]
I_{NCX}	Atrium<ventricle (-30%)[60] $k_{d,act}$ increased by 50%	Upregulated in cAF (+40%) [17, 25, 61, 62]	Unchanged
SERCA	No changes in maximal pump rate K_{mf} increased 2-fold [1742, 63]	Reduced maximal pump rate [17]	Forward mode km reduced by 50% [57]
RyR	Unchanged	Increased sensitivity for luminal Ca (2-fold) [17, 61]	Sensitivity to $[Ca^{2+}]_{SR}$ enhanced twofold [57]
SR Ca^{2+} leak	Unchanged	Increased by 25%	Unchanged
TnI	Unchanged	Unchanged	Affinity for Ca^{2+} decreased [57]
I_{NKA}	Atrium<ventricle (-30%)[60]	Unchanged [64]	Affinity for $[Na^+]_i$ increased by 25% [65]